
Autoregressive Order Selection for Rotating Machinery

Suguna Thanagasundram[†] and Fernando Soares Schindwein

Department of Engineering, University of Leicester, University Road, Leicester LE1 7RH, UK

(Received 6 October 2005; accepted 17 May 2006)

This paper provides a practical rule for determining the minimum model order for Autoregressive (AR) based spectrum analysis of data from rotating machinery. The use of parametric methods for spectral estimation, though having superior frequency resolution than Fast Fourier Transform (FFT) based methods, has remained less favoured mainly because of the difficulties in estimating the model order. The minimum model order p_{\min} required is the ratio of the sampling rate and the rotating speed of the machine. This is the number of samples in one shaft revolution. Traditional model order selection criteria, Akaike Information Criterion (AIC), Finite Information Criterion (FPE), Minimum Description Length (MDL), Criterion Autoregressive Transfer-function (CAT), and Finite Information Criterion (FIC) are used to estimate the optimal order. These asymptotic criteria for model order estimation are functions of the prediction error and the optimal order of an AR model is chosen as the minimum of this function. Experimental results, using vibration data taken from a dry vacuum pump at different sampling rates and rotating speeds, show that at p_{\min} there is a marked reduction in the prediction error. For low speed rotating machinery, the optimal order is p_{\min} . As the speed of the rotating machine increases, there is some advantage in using twice or thrice p_{\min} , to produce more accurate frequency estimates. The Box-Jenkins method of order determination using autocorrelation and partial autocorrelations plots are also used for justification of the selection of this minimal order.

[†] Member of the International Institute of Acoustics and Vibration (IIAV)

1. INTRODUCTION

Fault detection and prognosis of equipment is an established technique in many industries worldwide today. Much of the equipment monitored, such as pumps, diesel engines, compressors, and electric motors, belong to the class of rotating machines and produce signals that are quasi-stationary time series. The reliability, availability, and maintainability of these machines are critical to the overall performance and operation of many companies for maintaining their competitiveness in a global marketplace. It is clearly important to receive warnings of problems before failure and outage occurs. Rotating machinery produces signals that are random processes. Examples of these are displacement measurements from proximity probes, vibrations from accelerometers, sound from acoustic emission sensors, and pressure signals from calibration gauges. Signals captured from rotating machines can be used as indicators of the equipment's health for fault prediction and prevention. One way of achieving this is to use time domain analysis,¹ where statistical parameters are computed and compared with baseline figures, as a change in these parameters may indicate imminent malfunction. An alternative approach is using frequency domain analysis,² where the spectra of the faulty signals are compared with a baseline spectrum obtained from machinery run in normal no-fault conditions.^{3,4}

Power Spectral Density (PSD) estimation is performed predominantly using classical techniques based on the Fast Fourier transform (FFT). The FFT is the favoured method for spectral analysis as it is well established and there are Commercial-Off-The-Shelf (COTS) products which aid the implementation of tools for frequency estimation of signals as part of larger condition monitoring programs for fault de-

tection in machines. An alternative class of frequency estimation methods is parametric modelling. The parametric approach is based on modelling the signal under analysis as a realisation of a particular stochastic process and estimating the model parameters from its samples. These methods are commonly used in seismic analysis, stock market forecasting, and in biomedical engineering.⁵ The usage of parametric spectral analysis for fault detection and condition monitoring of rotating machinery has remained low, mainly because the order of parametric models has to be determined beforehand to obtain good frequency estimates.

In recent years, there have been some investigators who have applied the technique of parametric modelling for condition monitoring investigations. Mechefske has employed parametric modelling for fault detection of bearing faults.⁶⁻⁸ Mechefske has noted that AR modelling is especially useful in low speed machinery, as recording long periods of data in slow speed machines is impractical and the AR method is particularly adequate in such cases, as it can work with short data records and achieve better resolution than the FFT method. He has acknowledged that finding the model order is the most critical step in parametric modelling and has to be accurately determined for power spectral density approximations. Dron⁹⁻¹² has studied the usage of an AR modelling for vibration analysis of a forming press for a conditional maintenance program. He has noted that parametric methods are particularly worthwhile in the early detection of faults, especially when two typical frequencies are close to each other. Also, he has acknowledged that the model order selection is one of the major problems encountered when implementing parametric spectrum analysis methods.

In a recent work in 2001, Wenyi Wang has effectively applied the Minimum Phase AutoRegressive (MPAR) approach

for detection and diagnosis of gearbox faults for a helicopter application at the Aeronautical and Maritime Research Laboratory (AMRL).^{13,14} In 2000, Fang Wen also applied autoregressive modelling techniques for fault detection using helicopter data.¹⁵ It was noted in both studies, that the model order selection was a crucial part of the investigations.

Clearly the problem of finding the model order is the biggest obstacle for any investigator who wants to apply parametric techniques for frequency estimation. None of the above mentioned researchers performed a detailed study comparing various different techniques for estimating the 'correct' AR model order. This is the main issue addressed in this paper. It is shown how the concern for finding the model order for signals captured from rotating machinery can be allayed to a certain extent by using the simple rule of thumb we propose. This is stated as $p_{\min} = f_s / f_{\text{machine}}$ where p_{\min} is the minimum AR model order, f_s is the sampling rate of the data, and f_{machine} is the rotating speed of the machine.

1.1. Problem Formulation

The testing environment for this study is a five-stage 'Roots and Claw' dry vacuum pump, which is a type of rotating machinery. Initial interest began in the project when AR modelling was used for spectral estimation of vibration signals acquired from the pump and a suitable model order had to be determined. Methods of order selection criteria such as the Akaike Information Criterion (AIC), Final Prediction Error (FPE), Minimum Description Length (MDL), Criterion Autoregressive Transfer-function (CAT), and Finite Information Criterion (FIC) were computed to find the true order.¹⁶ On fine-tuning the methods used in that study, new and interesting results were obtained. From the plots of order selection criteria, a remarkable trend was seen. Functions of all above-mentioned order selection criteria had a steep decrease at a certain order. This minimum order, p_{\min} , is a function of the sampling rate, f_s , and the rotating speed of the machine, f_{machine} . This behaviour was found to be repeatable at different sampling rates and different rotating speeds. The explanation is simply that the minimum model order corresponds to the number of samples collected over a full turn of the machine, that is, p_{\min} . The argument is supported by our results and suggests that p_{\min} can be used as an initial optimal order for parametric modelling. Most of the tests were carried using the vibration signals from an ADXL105 micromachined accelerometer.¹⁶ The vibration signals from this transducer are representative of a true AR process, as can be seen from their autocorrelation and partial autocorrelation plots. Experiments were repeated in the same test conditions using vibration signals obtained from the pump with a Brüel and Kjær (B&K) piezoelectric accelerometer. The statistical properties of these signals, mainly the autocorrelation plots, were different from the ADXL105 vibration signals. Though the B&K vibration signal had a higher signal to noise ratio (SNR) than the ADXL105 vibration signal, the B&K signal was not modelled as well by an AR process as it had an autocorrelation function which slowly decayed with time. Results for these B&K signals are referred to in detail later in the text.

The proposed method was also validated on ADXL105 vibration signals obtained from a bearing which had a single point defect on the inner race. Knowing the geometric dimensions of the ceramic bearings of the dry vacuum pump,

the characteristic bearing defect frequencies were calculated from standard formulae available from the reference.⁴ For instance, the BSF (Ball Spin Frequency), BPFO (Ball Pass Frequency of Outer Race), BPFI (Ball Pass Frequency of Inner Race), and FTF (Fundamental Train Frequency, also known as Cage Frequency) were estimated to be around 464, 363, 530 and 40 Hz respectively when the pump's running speed was set to 100 Hz (taking in account a slippage factor of 2-5%). Results for the inner race defect frequency are discussed in more detail at the end of the paper.

Using the simple rule proposed here, it is shown how the order of AR modelling can be easily determined for rotating machinery such as the dry vacuum pump. It is hoped that this may lead to increased interest for usage of AR modelling for spectral analysis of signals from rotating machinery for condition monitoring schemes.

2. THE CASE FOR THE AR METHOD

There are a number of practical considerations to take into account when choosing a spectral estimator. Some of these include its performance in terms of resolution, variance, and potential for real time application. Strictly speaking, the traditional FFT-based methods make the assumption the process is periodic and stationary. In practice, processes are not periodic and exhibit non-stationarity. The performance of FFT tools degrades when applied to non-stationary signals. One way to deal with non-stationary behaviour is to use Short Time Fourier Transform (STFT) or Wavelet analysis.¹⁷ These techniques are more applicable to transient signals. AR models exhibit superior performance for nonstationary signals¹⁸ than classical non parametric methodologies; and, since AR-based spectral analysis can produce better spectral estimates for short segments of data it is better able to characterise the time-varying behaviour of frequency estimates.

The maximum frequency resolution using FFT-based methods is of the form:

$$\Delta f = \frac{f_s}{N}. \quad (1)$$

For the AR power spectral density (PSD) estimator, the resolution of processes consisting of sinusoids in white noise¹⁹ is given by

$$\Delta f = \frac{1.03f_s}{p[\text{SNR}(p+1)]^{0.31}}. \quad (2)$$

The frequency resolution of the FFT technique Eq. (1) is inversely proportional to frame size. The frequency resolution of the AR based method Eq. (2) is a function of the model order, p and also the signal to noise ratio (SNR).⁵ The main limitation of the FFT method is that it does not work well for short data records and has a limited frequency resolution. Also, the AR technique can work with smaller sampling rates (f_s) compared to the FFT methods. All that is required is slightly more than Nyquist rate to produce good frequency estimates, while the FFT method may need six or seven times the Nyquist rate to achieve the same performance. Also, because AR PSD estimators do not assume periodicity, they do not exhibit spectral leakage behaviour which are inherent in the FFT-based methods that cause the side lobe phenomenon which can mask weaker signals.¹⁹

The main advantages of the FFT PSD are that it is computationally efficient. The processing requirement of the FFT method is proportional to $N \log_2 N$. The processing requirement of the AR method mainly depends on two factors: first, the estimation method implemented, and second, it is proportional to p^2 , the square of the model order. The Yule-Walker estimation method is computationally less expensive than the covariance or Burg method. However, it should be noted that even the Yule-Walker algorithm is slower than the FFT method. Schlindwein^{20,21} has estimated that the AR technique is slower than the FFT technique by a factor of 2.58 for the same sample size ($N = 256$) and processor (TMS320C25) using the Yule-Walker method. The main advantage of the AR approach comes from the fact that it can work with smaller sample sizes for the same resolution compared to the FFT method. Hence, the AR technique only requires a fraction of the samples that are required by the FFT method for the same resolution, and it may cost less in terms of computational cost as fewer samples are used. This is an advantage especially for real-time applications.

2.1. Autoregressive (AR) Model

In an AR model²² the current value of the series, $x(n)$, is expressed as a linear function of previous values plus an error term $e[n]$, as given by Eq. (3) below

$$x[n] = - \sum_{k=1}^p a_k x[n-k] + e[n], \quad (3)$$

where $e[n]$ is white noise with zero mean and variance σ^2 , p is the order of the model, and a_k are the autoregressive coefficients. Once the a_k coefficients of the AR model are known, $P_{AR}(f)$, the AR power spectrum is given by Eq. (4) where T is the sample period.

$$P_{AR}(f) = \frac{2\sigma^2 T}{\left| 1 + \sum_{k=1}^p a_k e^{-j2\pi f k T} \right|^2}. \quad (4)$$

3. AUTOCORRELATION FUNCTION (ACF)

The autocorrelation function (ACF) is a statistical measure of the dependence of the time series values at one time on the values at another time. The ACF of a discrete time series is simply the correlation of the process against a time-shifted version of itself. For the time series $x(n) = 1, 2, \dots, N$, Box and Jenkins²³ defined the autocorrelation as Eq. (5)

$$R_{xx}(k) = \frac{1}{N} \sum_{n=1}^{N-k} (x(n) - \overline{x(n)})(x(n+k) - \overline{x(n+k)}), \quad (5)$$

where $\overline{x(n)}$ is the mean of the time series. The normalised value of the autocorrelation is given by Eq. (6):

$$\text{ACF}(k) = r_k = \frac{R_{xx}(k)}{R_{xx}(0)}. \quad (6)$$

This definition is known as the 'biased' estimator of the ACF. If the term N is replaced by $N-k$ in Eq. (6), we have the 'unbiased' estimator. The biased estimator is generally

preferred as it tends to have a smaller mean square error and decays faster to zero than the unbiased estimator.²⁴

Box and Jenkins²³ suggested that the examination of the behaviour of the autocorrelation function (ACF) and the partial autocorrelation function (PACF) of a time series can give information on the identification of the right type of model for its analysis and also aid in the selection of the right model order. The plot of the ACF is an indication of the randomness in the data. The periodicity of a signal can also be seen in its ACF plot. If a signal contains a periodic component with period P , a peak in the curve occurs at integral multiples of P . The ACF for an AR(k) model has form of exponential decay or a damped sinusoid or a mixture of both.²³

3.1. Partial Autocorrelation Function (PACF)

It has been shown by Broersen²⁵ that the true order of the AR signal depends not only on the characteristics of the AR process but also on the method of parameter estimation used. In this study we have chosen the Yule-Walker method with the Levinson-Durbin recursion to find the AR coefficients.⁵ The Yule-Walker method produces a biased estimate of the residual variance; however, it has been shown that the effect of bias on order selection is negligible.²⁶ The Yule-Walker estimation method was chosen mainly for its processing speed.

The Yule-Walker method is based upon a set of linear equations which relate the parameters of an AR model with the autocorrelation sequence. If the order of the AR model is defined as p , the Yule-Walker equations allow computations of the $p+1$ model parameters (the p coefficients and the variance) from the $p+1$ autocorrelation coefficients by solving a set of $p+1$ linear equations.⁵

Partial autocorrelation function (PACF) is the normalised autocorrelation that remains at lag k after the effects of shorter lags ($1, 2, \dots, k-1$) have been regressively removed from the autocorrelation function at lag k .¹⁹ The partial correlation coefficients can be seen as negated autoregressive coefficients $-a_k$. The PACF helps to determine the order of the AR process. If a time series is an AR(k) process, then the PACF plot for the signal converges to zero for orders greater than k .

3.2. Confidence Interval

For a time series of N observations, Bartlett's approximation sets the 95% confidence region at $\pm 2/\sqrt{N}$.²³ These approximate confidence bounds provide limits to help judge the statistical significance of the AR parameters calculated. If a parameter is outside the confidence interval limit, then it can be concluded that the true order of the AR process has not been reached yet. Once they are within the limits, the residuals of the model are white and the true order has been reached.

4. ORDER SELECTION CRITERIA

The model order needs to be estimated as part of AR power spectral density estimation. The trade-off between resolution and variance is determined by the order in AR spectra. Usage of too low a model order results in highly smoothed spectra, masking the peaks of frequencies of interest. Conversely, usage of too high an order increases the

resolution and introduces spurious detail into the spectra because of spectral splitting. Spectral line splitting is a phenomenon observed as a result of two or more closely spaced peaks occurring in the spectral estimate where only one peak should have been present. This behaviour was first documented by Fougere.²⁷ He noted that extra poles were generated by additional AR parameters due to the usage of a higher order than required. This had given rise to the spurious peaks. Choosing a model with the smallest order that describes the true spectrum is an important principle in model selection and is referred to as the principle of parsimony. Estimation of the right order p is vital as usage of the wrong order for spectral estimation can produce incorrect frequency estimates.

Two of the order selection criteria used in this study to generate the prediction error plots are Akaike's Final Prediction Error (FPE)²⁸ and Akaike Information Criterion (AIC)²⁹. The third is Rissanen's Minimum Description Length (MDL) estimator³⁰ and the fourth is a method proposed by Parzen, the Criterion AR Transfer (CAT) Function³¹. These techniques for estimation of the AR order are termed 'asymptotic information criteria.' The performance of a more recent method of order selection criterion, Finite Information Criterion (FIC)²⁶ was also investigated. FIC has been claimed to perform better than asymptotic criteria when the ratio p/N is large. The FIC criterion is defined by Eq. (11) where $v_i = (N-i)/\{N(N+2)\}$ is the finite sample variance coefficient for the Yule-Walker method.

$$\text{AIC}(k) = \ln(\sigma(k)^2) + (2k+1)/N; \quad (7)$$

$$\text{FPE}(k) = \frac{N+k+1}{N-k-1} \sigma(k)^2; \quad (8)$$

$$\text{MDL}(k) = \sigma(k)^2 \left(1 + \left(\frac{p+1}{N} \right) \ln(N) \right); \quad (9)$$

$$\text{CAT}(k) = \left[\frac{1}{N} \sum_{j=1}^k \frac{N-j}{N\sigma(j)^2} \right] - \frac{N-k}{N\sigma(k)^2}; \quad (10)$$

$$\text{FIC}(k) = \ln(\sigma(k)^2) + 2 \sum_{i=1}^p v_i. \quad (11)$$

The difference between the mean square errors of the actual signal and estimated AR signal is termed the prediction error. The variance of prediction error of the AR model is defined as

$$\sigma(k)^2 = \frac{1}{N-p} \sum_{n=p+1}^N \left\{ x(n) + \sum_{i=1}^p a_i x(n-i) \right\}^2. \quad (12)$$

The optimal model order in each case is the order k that minimises the criterion given by Eqs. (7)-(11).

All these criteria were designed to reduce the probability of under-fit at the cost of over-fit.²⁵ They have a built-in penalty factor term in them which increases with increasing model order. The prediction error decreases with increasing model order. The order selection criteria achieves a minimal criterion value at the optimal model order. The criteria can only be used as guidelines for initial order selection. They are known to work well with computer generated synthetic AR

signals but may not work well with actual data, depending on how well such data can be modelled by an AR process.¹⁹

There has been a lot of work published in the medical field regarding the usage of model order selection criteria for AR-based spectral estimation. Schlindwein and Evans have applied AIC, FPE, and CAT model order criteria for spectral analysis of Doppler ultrasound signals²⁰ and concluded that overestimating the model order is better than underestimating it. They also noted that that using shorter frames (fewer samples) is more likely to produce an underestimation of the model order. Another researcher, Anita Boardman,³² has used most of the order selection criteria, as used in this investigation, to determine the optimum order for heart rate variability from the spread of orders in histogram plots. In a much more recent work in 2003,³³ electroenterograms recorded from the abdominal surface of Beagle dogs were used as test data for AR-based spectral estimation. In that study, many frames of data were analysed and the optimum order was chosen as the order which had the highest probability of having the minimum criteria values using the order selection criteria stated above.

The task of finding the optimum order is not trivial. The main difficulty arising from using the order selection criteria arises from the need to apply the criteria to a large number of frames of data. The optimum order cannot be determined by applying it to one frame of data alone because that frame of data might not be representative of the overall properties of the signal. Many frames of data of the signal have to be analysed before the optimum order can be determined accurately and conclusively. Some investigators work it out as probabilities, while others use more graphical methods, such as histograms. The process becomes rigorous with the requirement of the processing of orders for many frames of the signal.

Secondly, it is unwise to find the optimal order by the application of one order selection criterion alone. It has been reported by some researchers that certain criteria like FPE tend to overestimate the model order.¹⁰ In an earlier work by the authors, it was noticed that criteria like the MDL have the tendency to underestimate the model order.¹⁶ It is advised to test the performance of a combination of criteria, and if all them select the same minimum order then that order can be concluded to be the optimum order. It can be seen that the task of finding the optimum model order is tedious and difficult. The main motivation for this work is to overcome this problem, especially for rotating machines; and thus, establish a formulation for p_{\min} . The application of the p_{\min} method can ease the estimation of the minimum optimum order required for rotating machinery.

5. HARDWARE AND DATA ACQUISITION

This section contains a description of the test equipment and instrumentation used for obtaining the test signals used for the experiment. A multistage IGX dry vacuum pump based on the 'Roots and Claws' principle was used as the rotating machine. The schematic of the pump, the sensors used for capturing the data as well as set-up of the data acquisition system, is shown in Fig. 1. The speed of the pump, f_{machine} , was varied at a fixed 0 mbar loading factor and vibration signals were collected with different sampling rates. The theoretical values for p_{\min} were worked out for the various speeds and sampling rates and are given in Table 1.

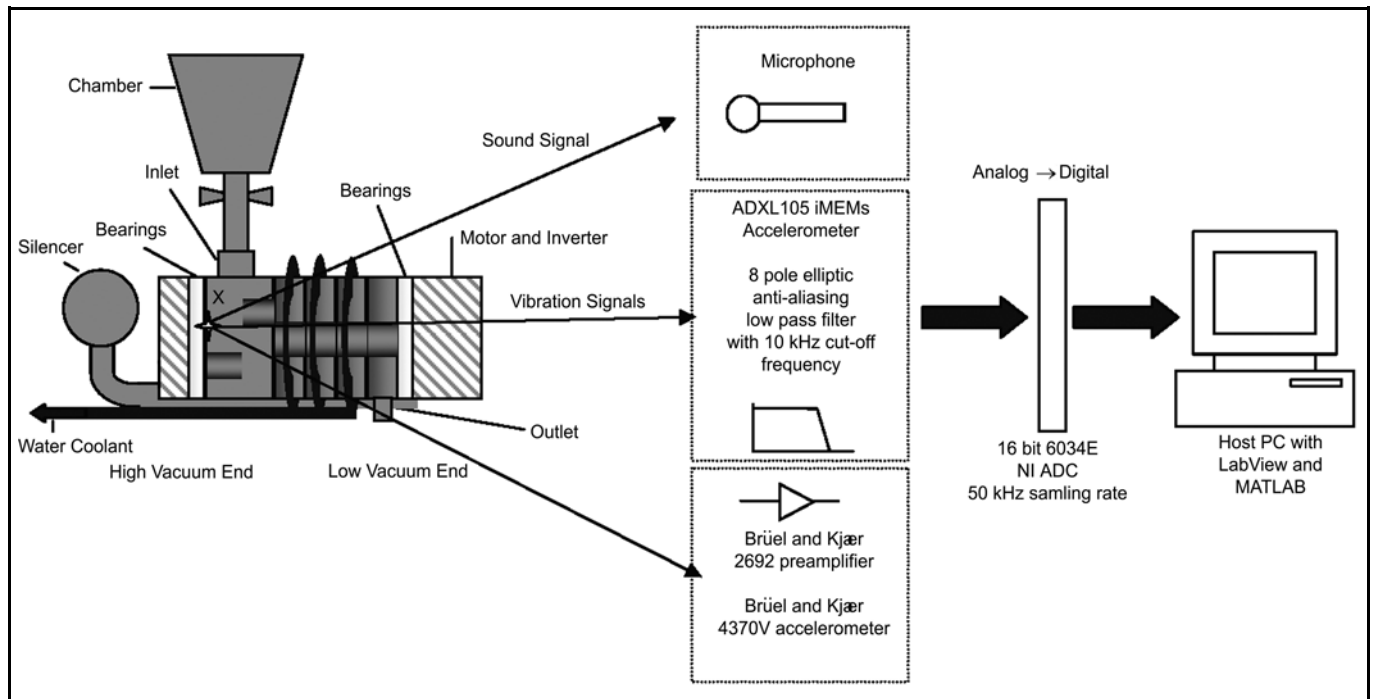


Figure 1. Schematic of the complete data acquisition system. The ADXL105 and Brüel and Kjær 4370V accelerometers were mounted radially on the pump near the high vacuum end to capture vibration signals. The microphone was attached in the vicinity of the high vacuum end.

Two different types of accelerometers were mounted radially on the pump near the high vacuum end to capture vibration signals. One is a surface micromachined accelerometer ADXL105. The other is a piezoelectric Brüel and Kjær (B&K) 4370V accelerometer. The signals from the ADXL105 accelerometer were filtered with a Low Pass (LP) filter custom built in our laboratory. The filter is an 8th order elliptic low-pass with a cut-off frequency of 10 kHz and attenuation of almost 70 dB in the stop band. The vibration signals from the Brüel and Kjær 4370V were conditioned using a Brüel and Kjær 2692 preamplifier that includes a 10 kHz LP filter. The analogue to digital conversion of the signals was performed with a 16-bit NI 6034E ADC card. The signals were sampled at 2 kHz because we knew that the fault frequencies lie in the range from 0-1 kHz for the pump speed set to 50-110 kHz. Varying lengths of the signals were used as per our requirements for determination of the minimum order. Most of the analysis done in the study was carried out using the ADXL105 vibration signals.

Table 1. $N_s = p_{\min} = f_s / f_{\text{machine}}$ shows the theoretical p_{\min} values which are the same as the number of sample points per revolution calculated for various rotating speeds and sampling rates.

f_{machine} (Hz)	f_s (Hz)	N_s (Number of sample points per revolution)
100	2000	20
100	4000	40
100	5000	50
60	2000	$33^{1/3}$
60	4000	$66^{2/3}$
60	5000	$83^{1/3}$

6. RESULTS AND DISCUSSION

6.1. ADXL Signal at Increasing Rotating Speed

Order selection criterion values were calculated using the AIC, FPE, MDL, CAT, and FIC equations (Eqs. (7)-(11)) for the vibration signals obtained from the pump using the ADXL105 accelerometer. When data was acquired for the analysis to generate the diagrams in Fig. 2, the speed of the pump, f_{machine} , was kept at 100 Hz. The sampling rate, f_s , was 2,000 Hz for Figs. 2(a)-(c). p_{\min} is 20 (refer to Table 1). Only the frame size N was varied. Looking at Fig. 2(a), it can be seen that the behaviour of all order selection algorithms was very similar. Initially they showed a dramatic drop in their criterion values. Then this decrease becomes more gradual. The point where this occurs is the p_{\min} order of 20. The criterion curves then flatten out and remain relatively constant until order 40 ($2p_{\min}$) is reached, where the curves for the 5th order selection criteria show another sudden decrease. A third slight decrease in the criterion values is again observed at $3p_{\min}$, at order 60. After order 60 there is no further 'step' decrease in prediction error.

From the above we can conclude that there is a relationship between the prediction error (all the order selection criteria are functions of the prediction error) and the number of samples per revolution N_s (which is the same as p_{\min}). It is expected of the prediction error of an AR model to decrease monotonically with the order, but looking at Fig. 2(a), we can clearly see that the decrease in prediction error has occurred in step changes at multiples of p_{\min} . For Figs. 2(b) and (c), the criterion values do begin to increase. This effect is more clearly seen in Fig. 2(c). This happened because the frame length was decreased from 4 to 1 and 0.25 s, respectively. The number of samples N used for the order selection estimation has an effect on the behaviour of the criteria. If the ratio

N/p is large, then the penalty factor inbuilt in each of these order selection criteria has a greater effect. This explains the increase in the values observed in Fig. 2(c) where a small frame size was used. So, clearly the order selection criteria are dependent on the number of samples. Even then, if one looks closely at Fig. 2(c), one can see small kinks occurring at 20, 40, and 60, which are multiples of p_{min} . If one were to choose an optimal order for AR modelling, looking at Figs. 2(a)-(c), one can say that the order cannot be less than 20, which is p_{min} . There might be an argument for choosing order 40 as there is a further slight decrease in the prediction error. Choosing an order above 60 is not worth the additional complexity as the small benefit of a better fit gained is not worth the large increase in the computational power required. Hence we can say that the ‘knee of the curve’ has occurred at order 20, and one may choose either order 20 or order 40.

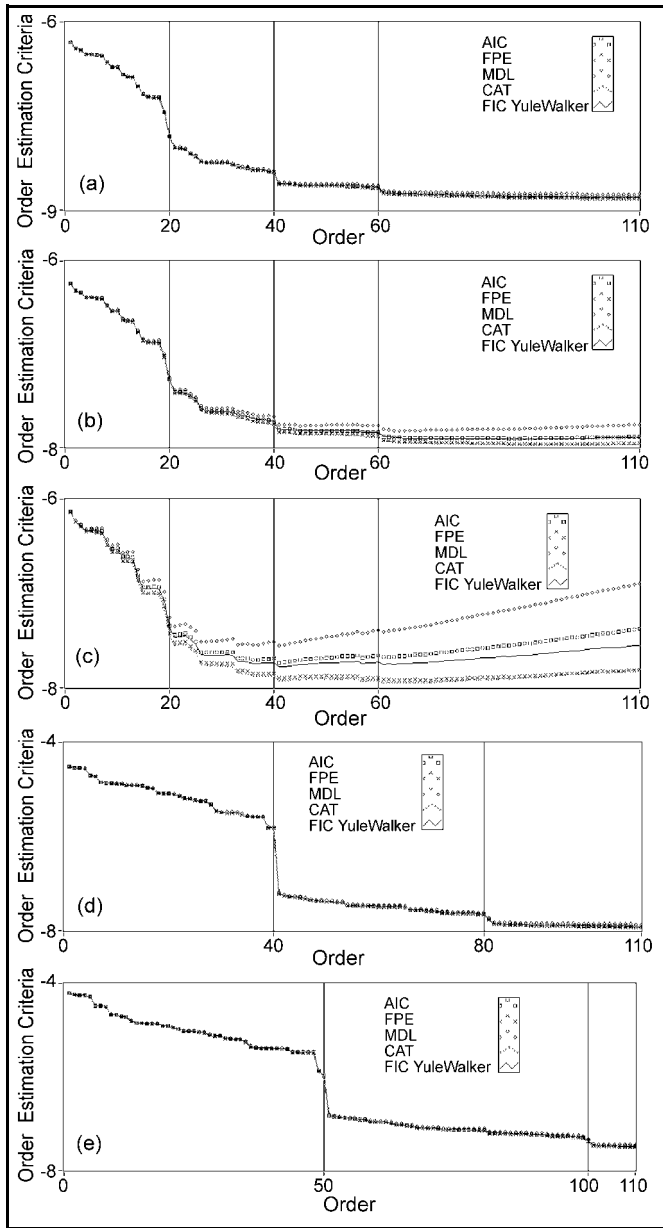


Figure 2. Behaviour of order selection criteria for analysis of ADXL105 vibration signals. The speed of pump $f_{machine}$ was fixed at 100 Hz. Sampling rate remained constant at 2,000 Hz but the length of frames was set at 4, 1 and 0.25 s, respectively, for figures (a) to (c) in that order. For (d) and (e) the length of frame was 4 s, but sampling rate was 4,000 Hz for (d) and 5,000 Hz for (e).

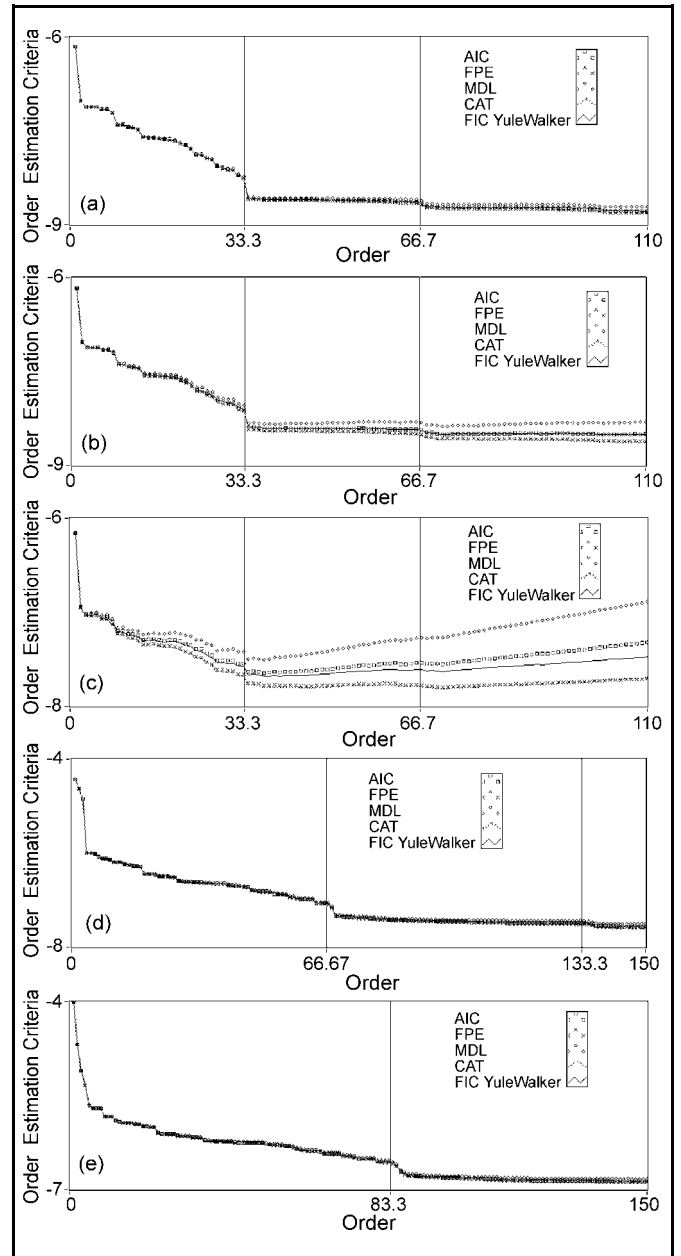


Figure 3. The speed of pump $f_{machine}$ was 60 Hz. Sampling rate f_s remained constant at 2,000 Hz, but the length of frames was set at 4, 1 and 0.25 s, respectively, for figures (a) to (c), in that order. For (d) and (e) length of frame was kept constant at 4 s, but sampling rate was 4,000 Hz for (d) and 5,000 Hz for (e).

When the sampling rate is increased to 4,000 and 5,000 Hz, the value of is 40 and 50, respectively. In Figs. 2(d) and (e), we can observe kinks occurring at multiples of 40 and 50, supporting the hypothesis. The speed of the machine $f_{machine}$ was decreased to 60 Hz and the same experimental procedure was repeated. The results are presented in Fig. 3. The same kind of analysis as that discussed above can be used to explain the results. However, there was one effect to be noted. The size of the steps in the prediction error changed with the speed of the machine. The drop in prediction error was much less for 60 Hz than for 100 Hz. The knee of the curve occurs at smaller multiples of the p_{min} value. Looking at Fig. 3(a), we can say that the knee of the curve has occurred at around 33 (the sampling rate was 2,000 Hz and speed of machine was 60 Hz). If one had no knowledge of the order selection criteria, we propose that the optimal order

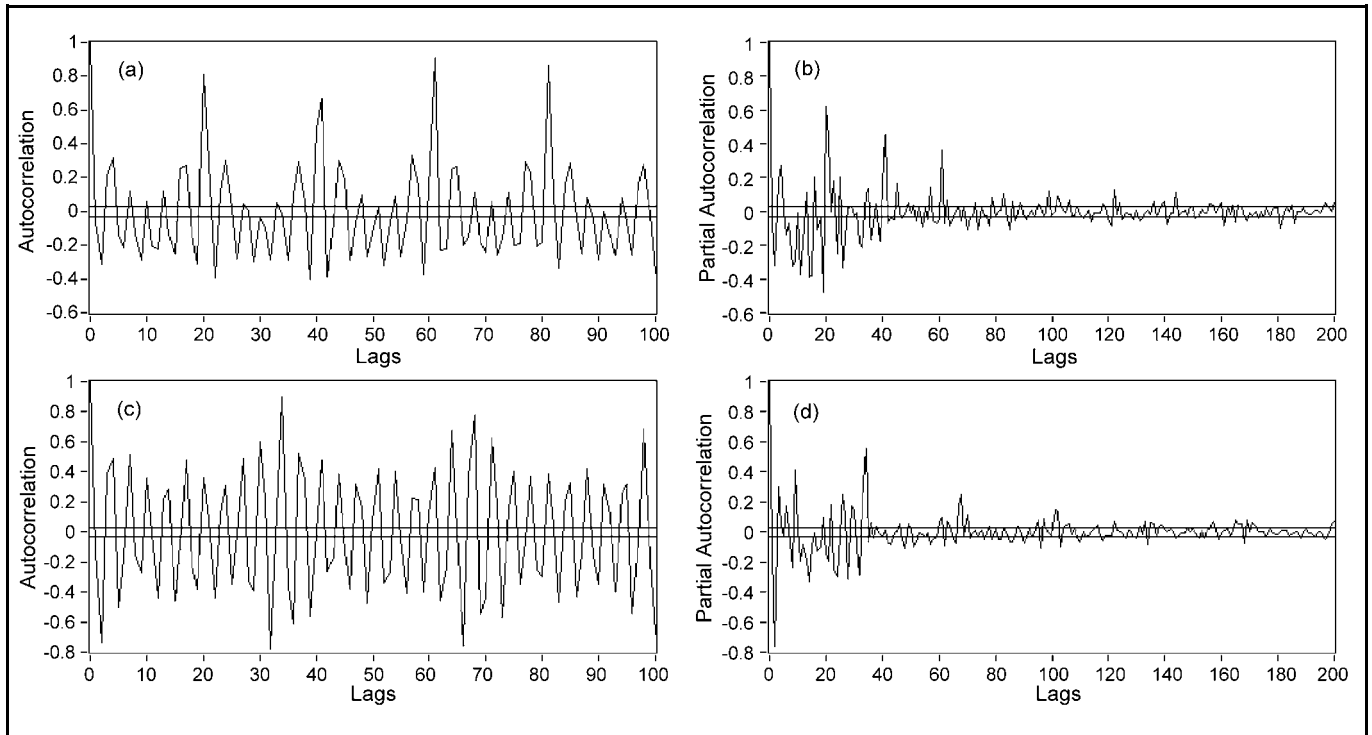


Figure 4. Speed of pump $f_{machine}$ was set at values as those indicated in the figures. ADXL105 vibration signal acquired at a sampling rate f_s of 2,000 Hz. Length of frames was 2 s. Horizontal lines denote 95% confidence interval level. (a) 100 Hz (ACF), (b) 100 Hz (PACF), (c) 60 Hz (ACF), and (d) 60 Hz (PACF).

could be estimated from the p_{min} formula because the order selection criteria also predict orders close to this value. It should be noted that if a higher speed of machine were used, then there would be some advantage in using twice or thrice p_{min} because of the characteristic behaviour we have observed.

6.2. ACF and PACF Plots for ADXL Signal at Increasing Rotating Speed

Statisticians use ACF and PACF plots to predict the model order of AR models. Figures 4(a) and (c) show the ACF plots of the vibration signals from the ADXL105 when the speed of the pump $f_{machine}$ was set to 100 and 60 Hz, respectively. The corresponding PACF plots are shown in Figs. 4(b) and (d). The periodicity of the pump can be clearly seen in the ACF plots. The repetitive peaks occur at 20 and 33.3, accordingly. Looking at Figs. 4(a) and (c), it can be seen that ACF has a periodic behaviour with the periods occurring at multiples of p_{min} . The envelope between the repetitive peaks is a decreasing exponential. It is to be noted that as the speed of the machine is increased, the process resembles more a true AR process. This can be seen in the well-defined ACF plot in Fig. 4(a). The order of the process is the point where the PACF plot cuts off. We have used the 95% confidence limit to judge the point where the function has died off. Referring to Fig. 4(b), we can see spikes occurring at 20, 40, and 60. At orders (or lags) above 60, the PACF becomes like white noise. The same behaviour is observed in Fig. 4(d). Here the spikes occur at multiples of 33.3. The amplitudes of the spikes decrease and there is a more marked decrease as the speed of the machine increases. An optimal order for Fig. 4(d) would be 33 and this is the p_{min} value for the vibration signal at that sampling rate and machine speed (refer to

Table 1). This is in line with the behaviour we observed with the order selection criteria plots.

6.3. ADXL Signal Spectrum

– Effect of Increasing Frame Length

This section explores the effect the frame length has on frequency resolution of the AR frequency estimates. We used the optimal model orders we had determined earlier using the order selection criteria and PACF plots and check whether they are the right orders required to model this ADXL vibration signal's basic behaviour. For Figs. 5 and 6, the speed of the pump, $f_{machine}$, was fixed at 100 Hz. The sampling rate, f_s , was 2,000 Hz. The only difference between Figs. 5 and 6 is that a frame length of 0.25 s was used for the former and 4 s for the latter. As the order was increased from 20 to 60, the resolution of the spectra improves. But as order is increased from 60 to 80, there is not much improvement in terms of resolution, but only a slight increase in the PSD variance. In fact, Figs. 5(c) and (d) look very similar. Hence, order 60 is sufficient for this machine speed and sampling rate. The Welch method, an averaged modified FFT periodogram, was used to obtain Figs. 5(e) and 6(e). A Hamming window and 50% overlap were used to obtain these frequency estimates. The frame size used was $N=500$ and 8,000 samples for Figs. 5(e) and 6(e), respectively. The sizes of the sections were 256 and 4,096 accordingly. There is a remarkable difference between the spectra in Figs. 5(e) and 6(e). The reason for this is that a much larger frame size N was used in Fig. 6(e) than in Fig. 5(e). Hence, the strong dependence of the FFT-based methods on frame size is clearly observed. It is well-known that FFT-based techniques require large frame sizes to provide accurate frequency estimates. AR-based techniques can work with smaller frame sizes, and hence, lead to an improvement in the time resolution.

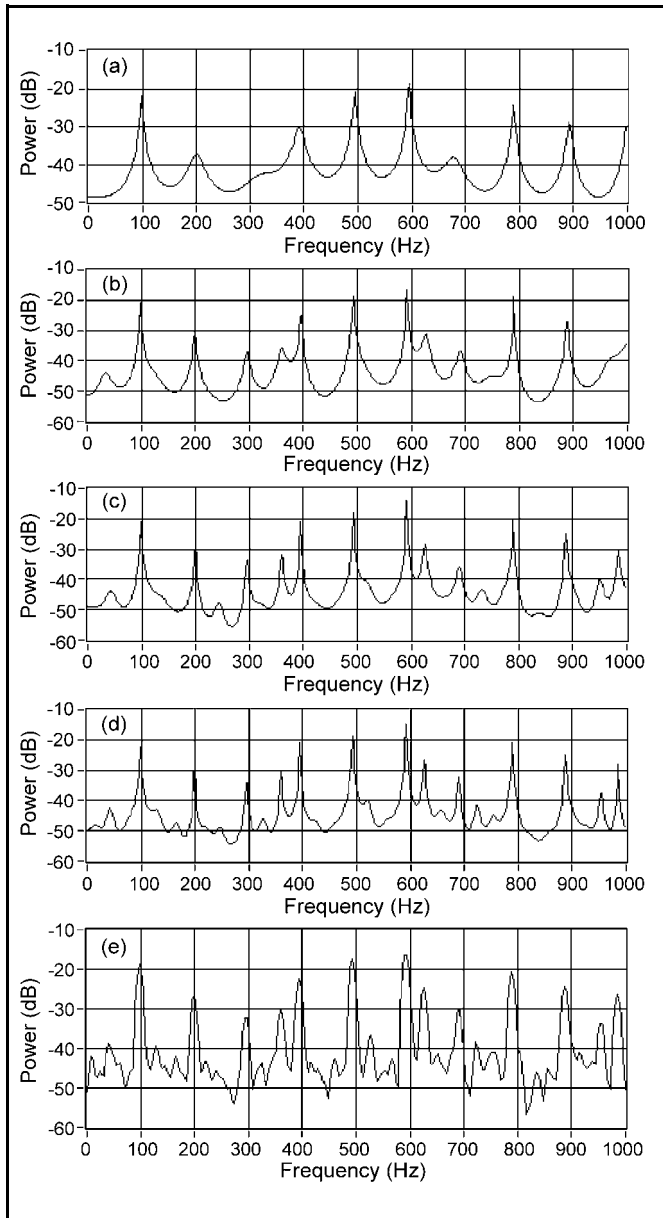


Figure 5. Spectra of ADXL105 vibration signal. Speed of pump $f_{machine}$ was 100 Hz. Sampling rate f_s was 2,000 Hz. Frame length was 0.25 s. Figures (a) to (d) show AR frequency estimates of order 20, 40, 60, and 80, respectively, (e) shows FFT frequency estimate obtained using the Welch method.

6.4. Brüel and Kjær (B&K) Vibration Signals at 100 and 60 Hz

Comparisons are also carried out with the Brüel and Kjær vibration signals. This accelerometer has a frequency response from 0 to 4,800 Hz and a smaller noise density specification of 0.02 mg/Hz (where g is the acceleration of gravity) compared to the ADXL105 accelerometer. The SNR of the vibration signal obtained using the Brüel and Kjær accelerometer is higher than that of the ADXL vibration signal. It was investigated whether the proposed technique would also work with this signal. Results are shown in Figs. 7 and 8. The same behaviour is observed. Our formulation for where the optimal order would occur also works for this signal. But the decrease in prediction error at multiples of p_{min} is less marked, as the SNR of this signal is higher. Also, the Brüel

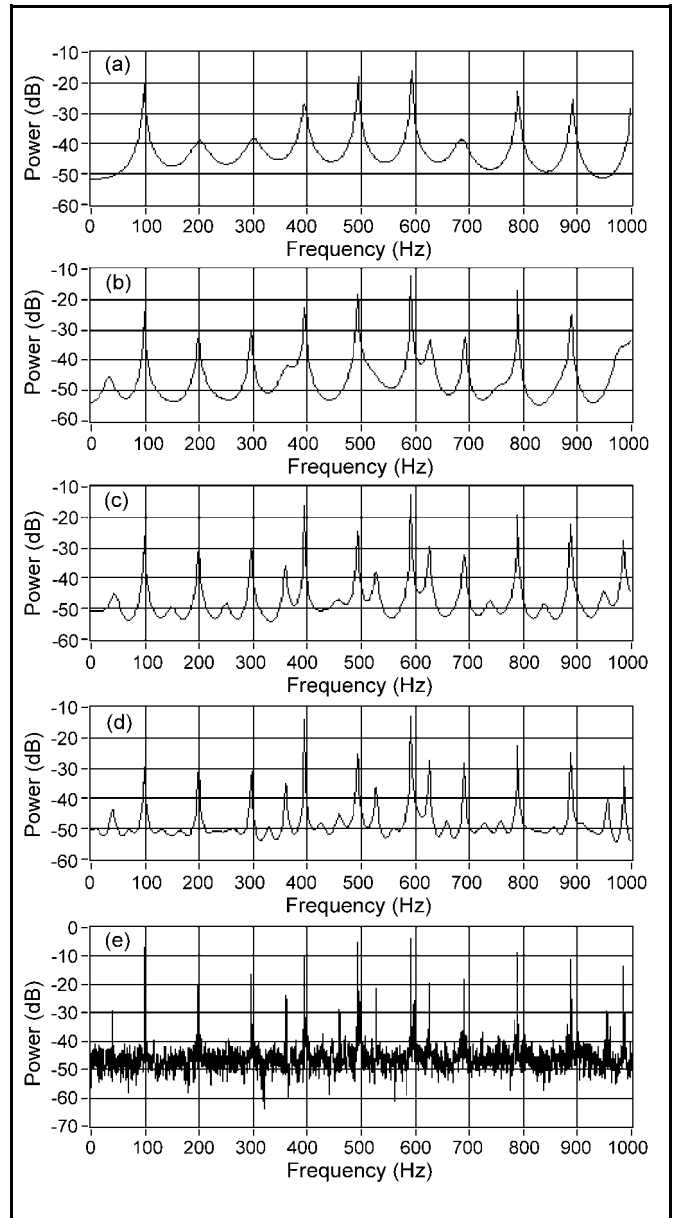


Figure 6. Spectra of ADXL105 vibration signal. Speed of pump $f_{machine}$ was 100 Hz. Sampling rate f_s was 2,000 Hz. Frame length was 4 s. Figures (a) to (d) show AR frequency estimates of order 20, 40, 60, and 80, respectively, (e) shows FFT frequency estimate obtained using the Welch method.

and Kjær vibration signals are not modelled as well by the AR process because they have a slowly decaying ACF function (Fig. 7(b)). For 100 Hz, the optimal order is at 40 ($2p_{min}$) as the speed of the machine was high, and at 60 Hz, the optimal order is exactly at p_{min} .

6.5. ADXL Results from a Signal with an Inner Race Fault

The proposed method was validated with ADXL105 vibration signal obtained from the pump fitted with a bearing which had an inner race fault. Spectra were plotted for the signal using both AR and FFT techniques (Fig. 9) for frame sizes of $N=400$ samples. In order to aid fault detection, the ADXL105 vibration signal from the faulty bearing was demodulated prior to spectral estimation using High Frequency Resonance technique (HFRT)³⁴ to strengthen the weak impulse

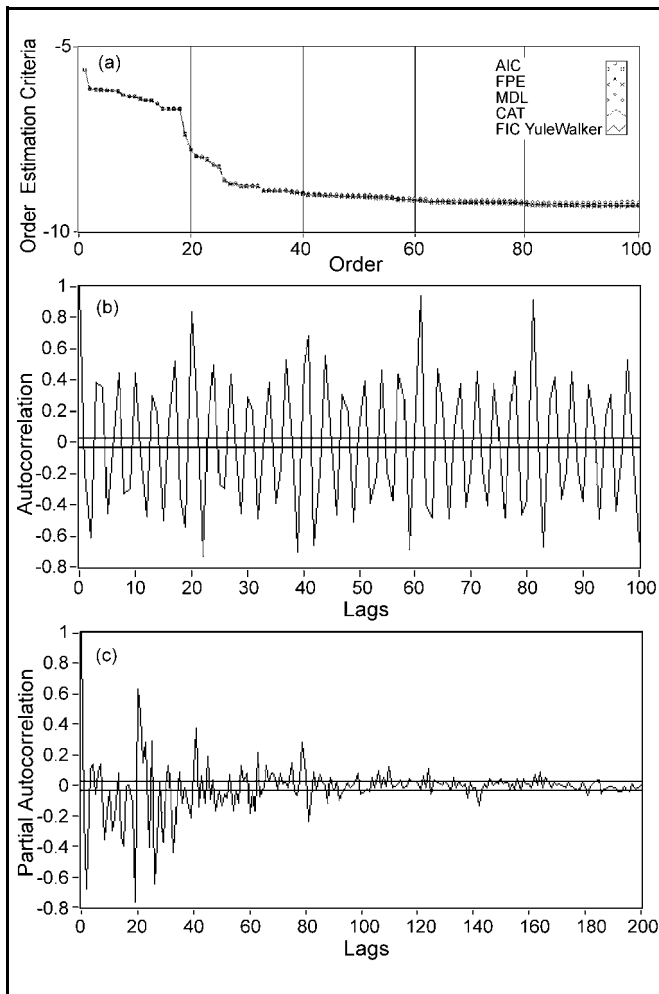


Figure 7. Vibration signal from Brüel and Kjær (B&K). Speed of pump $f_{machine}$ was 100 Hz. Sampling rate f_s was 2,000 Hz. Frame length was 2 s. (a) Order selection criteria, (b) ACF plot, and (c) PACF plot.

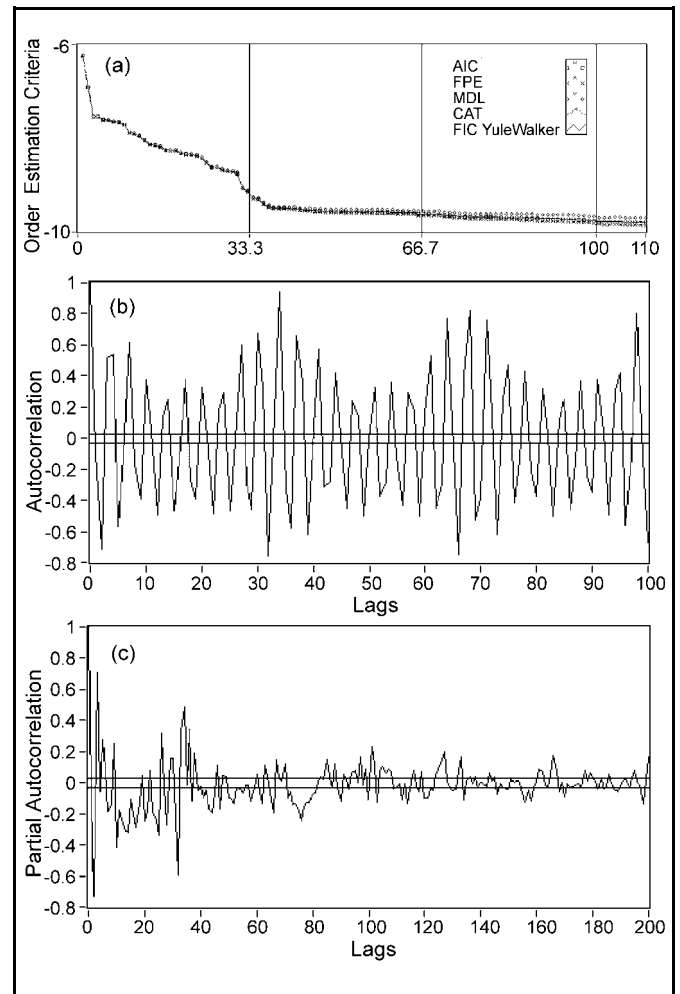


Figure 8. Vibration signal from Brüel and Kjær (B&K). Speed of pump $f_{machine}$ was 60 Hz. Sampling rate f_s was 2,000 Hz. Frame length was 2 s. (a) Order selection criteria, (b) ACF plot, and (c) PACF plot.

signals which are typical of bearing faults. The inner race defect frequency (BPFI) of 530 Hz is clearly evident in both FFT and AR spectra. For the AR spectra, a model order of 20 was used. This was equivalent to its p_{min} value and the signal $f_{machine}$ was 100 Hz. The sampling rate f_s was 2,000 Hz. The AR model order estimated by the p_{min} formula was sufficient to encapsulate the behaviour of the signal captured from a bearing fault and it can be seen that this method also works well on these faulty signals.

7. CONCLUSIONS

This paper presented a simple way of finding the optimum order for an AR model for the analysis of data from rotating machinery and justified the claim with experimental testing in several situations. The suggested AR model order $p_{min} = f_s / f_{machine}$ is the number of sample points corresponding to one shaft revolution. This finding is not surprising as the AR model can be seen equivalent to the standard multiple linear regression model. A current sample of the signal is estimated as a linear summation of p previous samples, where p is the model order. Hence, the number of samples used for the regression must be equal to at least the number of samples

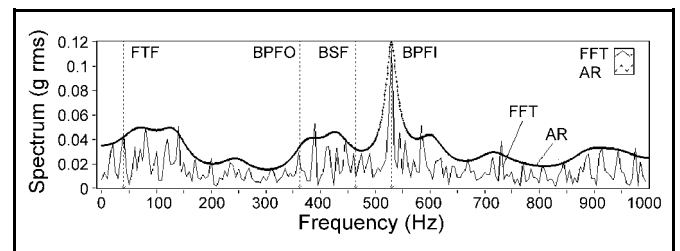


Figure 9. Spectra for ADXL105 vibration signal obtained from a bearing with inner race fault. Speed of pump $f_{machine}$ was 100 Hz. Sampling rate f_s was 2,000 Hz. A sample size of $N = 400$ samples was used. Spectra plotted using both AR and FFT techniques. The BPFI (Ball Pass Frequency of Inner Race) is clearly evident in both spectra. A model order of 20 was used for the AR spectra as suggested by the p_{min} value.

in one complete revolution of the signal for the prediction error to be low. This is the minimal model order.

Results show that the method is an excellent indicator of what the initial order should be. From the results presented the following concluding remarks can be made:

1. AR modelling can be used for spectral analysis in condition monitoring mainly because of its ability to work with smaller frame sizes and yet achieve a resolution improvement compared to FFT techniques.

2. AR modelling can be effectively used for fault diagnosis as the optimal order can be found easily with the formula p_{\min} we have proposed here.
3. This simple rule of thumb does not replace traditional order selection criteria, but can be used as a ballpark minimum figure for the optimal order.
4. It was noticed that as the speed of the machine increases, it might be advantageous to use twice or thrice the p_{\min} order.
5. This formula also works with signals with different SNR.
6. In this work, the AR model was constructed for a test environment with a fixed loading factor. If there are changes in the loading factor, it is anticipated that the performance of the proposed technique still remains the same. The calculation of p_{\min} still applies as increasing the loading factor of the pump only increases the level of the strength of the vibration felt by the pump. The number of basic harmonics of the fundamental shaft frequency in the AR spectra remains the same, hence, the minimum order is also expected to be the same.

REFERENCES

- ¹ Alfredson, R. J. and Mathew, J. Time domain methods for monitoring the condition of rolling element bearings, *Mechanical Engineering Transactions - Institution of Engineers*, **10** (2), 102-107, (1985).
- ² Alfredson, R. J. and Mathew, J. Frequency domain methods for monitoring the condition of rolling element bearings, *Mechanical Engineering Transactions - Institution of Engineers*, **10** (2), 108-112, (1985).
- ³ Mathew, J. Machine condition monitoring using vibration analyses, *Acoustics*, **15** (1), 7-13, (1987).
- ⁴ McNerny, S. A. and Dai, Y. Basic vibration signal processing for bearing fault detection, *IEEE Transactions on Education*, **46** (1), 149-156, (2003).
- ⁵ Kay, S. M. and Marple, S. L. Spectrum analysis - A modern perspective, *Proceedings of the IEEE*, **69** (11), 1380-1419, (1981).
- ⁶ Mechefske, C. K. Machine condition monitoring: Part 1 - optimum vibration signal lengths, *British Journal of Non-Destructive Testing*, **35** (9), 503-507, (1993).
- ⁷ Mechefske, C. K. Machine condition monitoring: Part 2 - the effects of noise in the vibration signal, *British Journal of Non-Destructive Testing*, **35** (10), 574-579, (1993).
- ⁸ Mechefske, C. K. and Mathew, J. Parametric spectral estimation to detect and diagnose faults in low speed rolling element bearings: Preliminary investigations, *Mechanical Systems and Signal Processing*, **7** (1), 1-12, (1993).
- ⁹ Dron, J. P., et al. Fault detection and monitoring of a ball bearing benchtest and a production machine via autoregressive spectrum analysis, *Journal of Sound and Vibration*, **218** (3), 501-525, (1998).
- ¹⁰ Dron, J. P., et al. High-resolution methods in vibratory analysis: Application to ball bearing monitoring and production machine, *International Journal of Solids and Structures*, **38** (24-25), 4293-4313, (2001).
- ¹¹ Dron, J. P., Bolaers, F., and Rasolofondraibe, L. Improvement of the sensitivity of the scalar indicators (crest factor, kurtosis) using a de-noising method by spectral subtraction: Application to the detection of defects in ball bearings, *Journal of Sound and Vibration*, **270** (1), 61-73, (2004).
- ¹² Dron, J. P., Bolaers, S. F., and Rasolofondraibe, I. Influence of the de-noising method by spectral subtraction on the diagnosis of rolling bearings, *European Journal of Mechanical and Environmental Engineering*, **48** (1), 3-12, (2003).
- ¹³ Wang, W. Linear model identification for gear fault detection using higher order statistics and inverse filter criteria, *Proceedings of the Sixth International Symposium on Signal Processing and its Applications*, **1**, 371-374, (2001).
- ¹⁴ Wang, W. Identification of gear mesh signals by kurtosis maximisation and its application to CH46 helicopter gearbox data, *Proceedings of the 11th IEEE Signal Processing Workshop on Statistical Signal Processing*, 369-372, (2001).
- ¹⁵ Fang, W., Willett, P., and Deb, S. Condition monitoring for helicopter data, *IEEE International Conference on Systems, Man and Cybernetics*, **1**, 224-229, (2000).
- ¹⁶ Thanagasundram, S., Abou Rayan, I. S. M., and Schlindwein, F. S. A case study of auto-regressive modelling and order selection for a dry vacuum pump, *Proceedings of the Twelfth International Congress on Sound and Vibration*, Lisbon, Portugal, (2005).
- ¹⁷ Guler, I., Hardalac, F. and Erol, F. S. Comparison of FFT, AR and wavelet methods in transcranial Doppler signal obtain from intracerebral vessels, *Proceedings of the 23rd Annual International Conference of the IEEE Engineering in Medicine and Biology Society*, **2**, 1832-1834, (2001).
- ¹⁸ Zhuge, Q., Lu, Y., and Yang, S. Non-stationary modelling of vibration signals for monitoring the condition of machinery, *Mechanical Systems and Signal Processing*, **4** (5), 355-365, (1990).
- ¹⁹ Lawrence Marple Jr., S. *Digital Spectral Analysis with Applications*, Prentice-Hall Inc., (1987).
- ²⁰ Schlindwein, F. S. and Evans, D. H. Selection of the order of autoregressive models for spectral analysis of Doppler ultrasound signals, *Ultrasound in Medicine & Biology*, **16** (1), 81-91, (1990).
- ²¹ Schlindwein, F. S. and Evans, D. H. A real-time autoregressive spectrum analyzer for Doppler ultrasound signals, *Ultrasound in Medicine & Biology*, **15** (3), 263-272, (1989).
- ²² Makhoul, J. Linear Prediction: A Tutorial Review, *Proceedings of the IEEE*, **63** (4), 561-580, (1975).
- ²³ Box, G. E. P., Jenkins, G. M., and Reinsel, G. C. *Time Series Analysis: Forecasting and Control*, Prentice Hall, 3rd edition ed, (1994).
- ²⁴ Jenkins, G. M. and Watts, D. G. *Spectral Analysis and its Applications*, Holden-Day series in time series analysis, (1968).
- ²⁵ Broersen, P. M. T. Finite sample criteria for autoregressive order selection, *IEEE Transactions on Signal Processing*, **48** (12), 3550-3558, (2000).
- ²⁶ Broersen, P. M. T. and Wensink, H. E. On finite sample theory for autoregressive model order selection, *IEEE Transactions on Signal Processing*, **41** (1), 196-204, (1993).
- ²⁷ Fougere, P. F., Zawalick, E. J., and Radoski, H. R. Spontaneous line splitting in maximum entropy power spectrum analysis, *Physics of The Earth and Planetary Interiors*, **12**, 201-207, (1976).
- ²⁸ Akaike, H. Fitting autoregressive models for prediction, *Annals of the Institute of Statistical Mathematics*, **21**, 243-247, (1969).
- ²⁹ Akaike, H. A new look at the statistical model identification, *IEEE Trans. Autom. Control*, **19**, 716-723, (1974).
- ³⁰ Rissanen, J. Universal coding, information prediction and estimation, *IEEE Trans. Inf. Theory*, **30**, 629-636, (1984).

- ³¹ Parzen, E. Multiple time series: determining the order of approximating autoregressive schemes, No 23, Statistical Sciences Division, State University of New York, Buffalo, NY, (1975).
- ³² Boardman, A., et al. A study on the optimum order of autoregressive models for heart rate variability, *Physiological Measurement*, **23** (2), 325-36, (2002).
- ³³ Moreno-Vazquez, J. J., et al. Autoregressive spectral analysis of electroenterogram (EEnG) for basic electric rhythm identification, *Proceedings of Annual International Conference of the IEEE Engineering in Medicine and Biology*, Institute of Electrical and Electronics Engineers Inc., Cancun, Mexico, (2003).
- ³⁴ Prashad, H., Ghosh, M., and Biswas, S. Diagnostic monitoring of rolling-element bearings by high-frequency resonance technique, *ASLE Transactions*, **28** (4), 439-448, (1985).